

Velocity Structure Near the Northern Manila Trench: an OBS Refraction Study

Allen T. Chen¹ and Yung-Sen Jaw¹

(Manuscript received 15 September 1995, in final form 25 July 1996)

ABSTRACT

A series of ocean-bottom seismograph experiments were conducted to establish velocity models in the southwestern offshore area of Taiwan from 1992 to 1993. Although the newly established system is still in its early stages, the data collected make it possible to define a crustal structure in the vicinity of the northern Manila Trench. The arrivals of deep refraction with apparent velocity at about 8.1 km/sec help to define the depth of the Moho discontinuity which is about 12 km below sea level. A thin crust of merely 5 to 6 km in thickness underlying the sediments to the west of the trench in the study area suggests an oceanic origin of the crust there. The thickness of the sediments is maintained over 3 km throughout the area, but a thicker crust to the east of the trench than that to the west is demonstrated.

(Key words: Ocean-Bottom seismograph, Velocity structure, Manila Trench)

1. INTRODUCTION

Located at the boundary between the Eurasian and Philippine Sea plates, the island of Taiwan, including its surrounding areas, is one of the most perplexing regions in the world in terms of tectonic complexity (Figure 1). Because many key structural features of the offshore region are covered with thick sediments and have not been fully investigated, several conflicting hypotheses regarding the northern extension of the Manila Trench have been proposed but have not been backed up with solid data. For instance, Biq (1977) proposed that the trench might run northward near 20.5°N and extend onshore through Fongliao Canyon in southern Taiwan; Lin and Tsai (1981) argued that it might terminate somewhere near 21°N and shift eastward to 121°E by a transform fault parallel to 21.2°N approximately. Recently, Lundberg *et al.* (1991) suggested that on the basis of six-channel seismic data acquired in offshore southern Taiwan the Manila Trench extends northward to at least 22.5°N. It might turn northeasterly there and further connect to the major thrust fault near Tainan (Huang *et al.*, 1992) or turn to the northeast near 22°N and continue its onshore extension to the Meilin thrust fault near Kaohsiung (Lee *et al.*, 1993). The different scenarios regarding the northern extension of the trench demonstrate only a small portion of the geological problems and complexities

¹Institute of Applied Geophysics, National Taiwan Ocean University, Keelung, Taiwan, R.O.C.

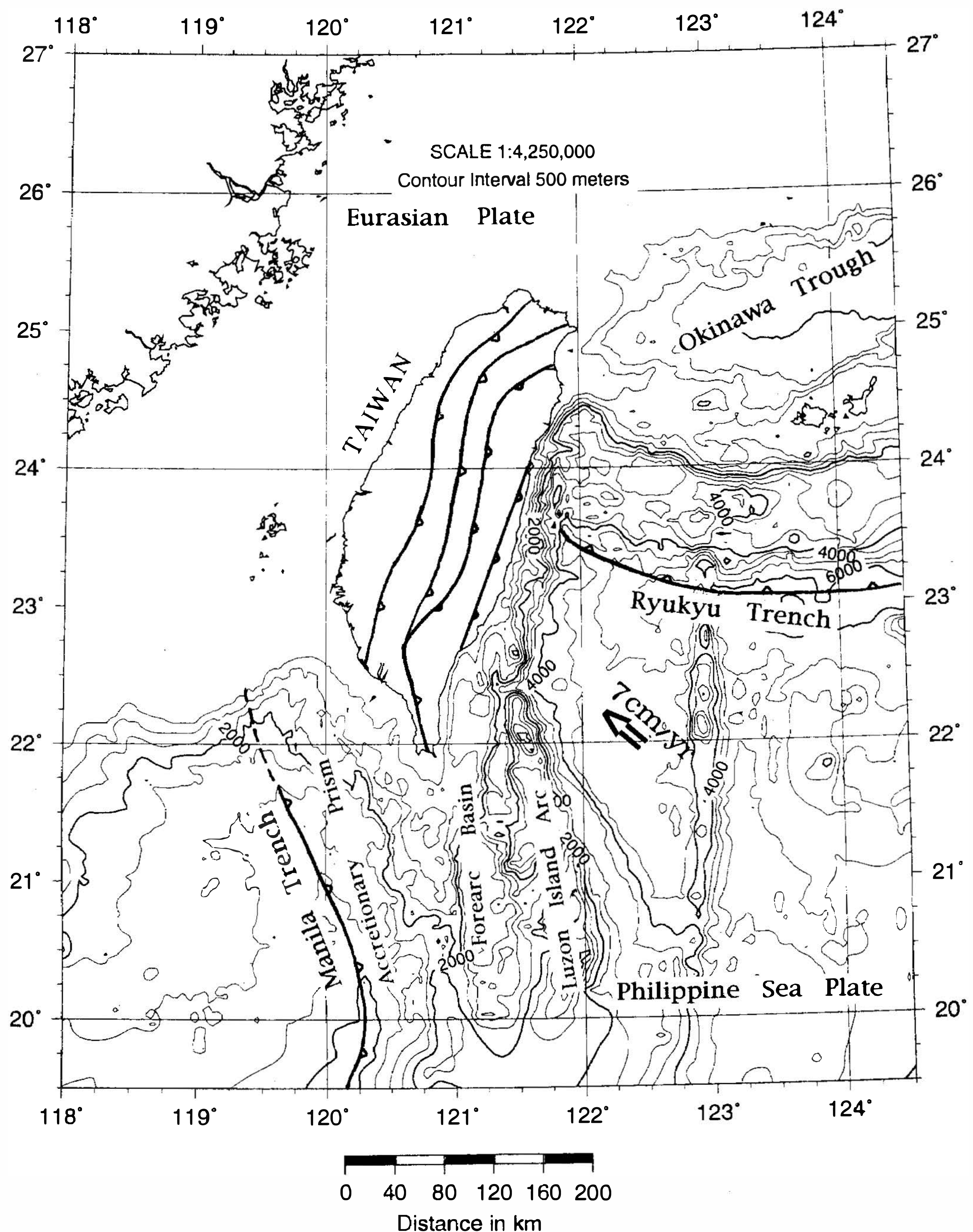


Fig. 1. Regional map of Taiwan and its surrounding area. Taiwan is located at the plate boundary between the Eurasian and Philippine Sea plates. The Philippine Sea plate moves northwestward at about 7 cm/year relative to the Eurasian plate. Bathymetric data are provided by C. S. Liu (*Liu et al.*, 1996).

pertaining to this convergent zone. In order to trace the trench and delineate the plate boundary between the South China Sea Basin and the Philippine block in southwestern offshore Taiwan (Seno and Kurita, 1978), the sedimentary and crustal structures would have to be established first. A study of the crustal structure can provide information to answer some basic questions. For example as what is the nature of the crust in southwestern offshore Taiwan? Is it oceanic as part of the South China Sea Basin, or continental, as part of the Eurasian plate? How is the tectonic evolution of Taiwan related to this part of the trench where subduction disappears and collision takes place? A spectacular relationship of plate movement enhances the enigma of geometric configuration: while a portion of the Eurasian plate-the South China Sea Basin is subducting eastward along the Manila Trench, the Philippine Sea plate maintains its subduction rate of 7 cm/year northwestward underneath the Ryukyu Trench.

Earthquake studies near the Manila Trench (Lin and Tsai, 1981) need further refining so that location ambiguity caused by the incomplete coverage by a seismic network confined on land can be resolved. Other geophysical means, such as gravity and magnetics have provided some estimates as to the depth to the magnetic basement , yet neither have they detailed the structure nor qualified the nature of the crust (e.g., Liu *et al.*, 1992). Multi-channel seismic profiling aimed at the deep structures in this region was not established until after the 1996 TAICRUST (Taiwan International Collaborative Research for Understanding Subduction-collision system in Taiwan) survey when *R/V Maurice Ewing* conducted a seismic survey covering the areas eastern and southern offshore Taiwan. However, those results have not been released yet. On the other hand, deep-penetrating, large-offset offshore seismic experiments using ocean-bottom seismographs (OBS) had already been carried out a few years before the TAICRUST.

OBS experiments were conducted from 1991 to 1993 in offshore Taiwan during the *R/V Ocean Researcher I* cruises 277, 282, 312 and 347, hereafter referred as ORI-277, ORI-282, ORI-312 and ORI-347, respectively (Chen *et al.*, 1992). The large-offset seismic lines that are presented here ran either across or parallel to the presumed northern extension of the Manila Trench between latitudes 21° and 22°N (Figure 2). These surveys were limited in both the number of instruments used and in the capacity of the seismic sources available. However, preliminary results provide some constraints to construct velocity models and reveal some interesting properties of the crustal structure.

2. TECTONIC SETTING

Under the framework of plate tectonics, the Eurasian plate interacts with the Philippine Sea plate at a convergent rate of about 7 cm/year along a southeast-northwestern direction (Seno, 1977; Seno and Kurita, 1978; Yu and Chen, 1994). The oblique collision of these two plates has caused intensive folding and severe faulting of the Taiwan mountain belt, thus resulting in one of the most rapid uplift rates in the world (Wu, 1978; Jahn *et al.*, 1986; Barrier and Angelier, 1986). Further to the south, however, an accretionary prism 70-110 km wide to the east of the Manila Trench (e.g., Bowin *et al.*, 1978; Suppe, 1988; Huang *et al.*, 1992; Reed *et al.*, 1992) is bounded by an incipient collision along the North Luzon Trough (Reed *et al.*, 1992). Based on the study of slip vectors of shallow earthquake events along the eastern margin of the Philippines, Seno (1977) proposed that the Philippine block is a microplate

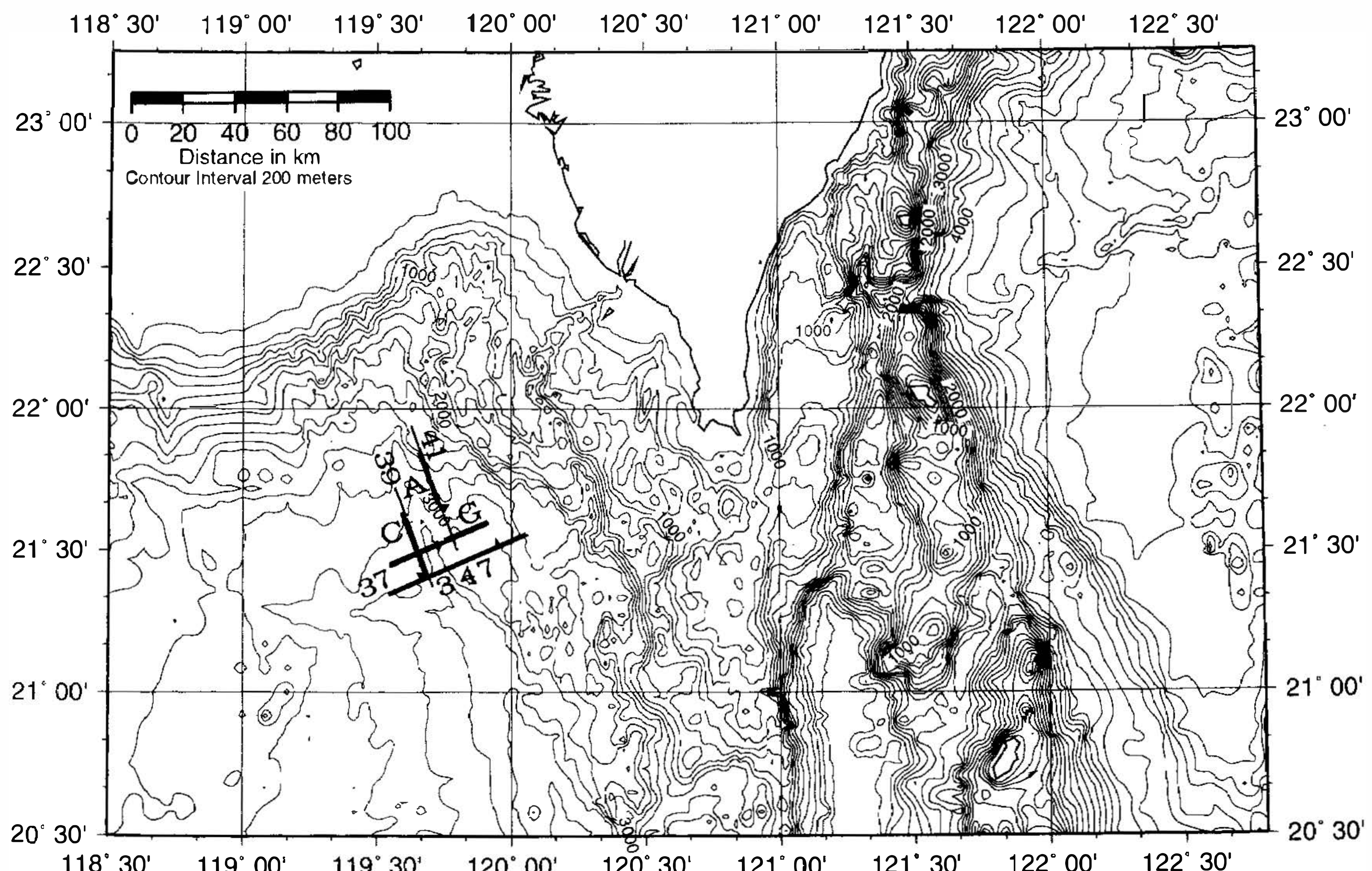


Fig. 2. OBS survey lines in offshore southern Taiwan, where A, C, G and 347 shown with thick lines represent survey lines ORI-312A, -312C, -312G and -347, respectively. Available multi-channel seismic lines MCS320-37, -39 and -41 are also shown with thin lines. Locations of the OBS (\blacktriangle) did not exactly fall on the survey lines. Bathymetric data are provided by C. S. Liu (Liu *et al.*, 1996).

sitting to the east of the Eurasian plate. The Manila Trench represents the boundary between the South China Sea Basin and the Philippine block. The South China Sea Basin is being subducted underneath the Philippine block. The Manila Trench can be recognized south of 21°N , but its topographic expression loses its characteristic features further north because of the change in the nature of the tectonic contact has from subduction to arc-continent collision (Biq, 1973; Suppe, 1988).

3. DATA ACQUISITION

The instruments (OBS) used in the experiments of this study were duplicated from the Texas OBS (Nakamura *et al.*, 1987; Chen *et al.*, 1994). Unfortunately, because of a failure to recover one of the two OBSs deployed in cruise ORI-312, and a loss of another set of data due to a tape recording problem in one of the OBSs deployed in cruise ORI-347, no reversed profile data were acquired. ORI-312G, however, was equivalent to a split spread line. The coordinates and water depths of each OBS deployed and data successfully analyzed, are shown in Table 1.

Table 1. OBS survey data.

Line	Coord. of End Points		OBS Location	Water Depth
ORI-312A	21°35.00'	119°45.40'	21°39.02' 119°44.99'	2928 M
			21°50.57' 119°39.91'	
ORI-312C	21°21.55'	119°42.25'	21°24.52' 119°39.92'	3153 M
			21°42.99' 119°33.57'	
ORI-312G	21°26.67'	119°33.15'	21°31.00' 119°43.97'	3116 M
			21°35.82' 119°54.97'	
ORI-347	21°20.32	119°32.81'	21°30.82 119°58.15'	3042 M
			21°33.27' 120°03.75'	

The size of the air-gun source varied on each cruise; an air-gun array of 15.1 liters (920 in³) in total volume was used on ORI-312, while a two-gun array with a total volume of 16.5 liters (1000 in³) was used on ORI-347. The air gun was shot at 30-second intervals while cruising at about 5 knots, giving a shot spacing of about 80 m. The survey lines ran through water depths ranging from 1800 m to 3600 m. While ORI-312G and ORI-347 were approximately perpendicular to the postulated extension of the Manila Trench, ORI-312A and -312C were parallel to it (Figure 2). The Global Positioning System (GPS) (Ashtech XII GPS) was used primarily for navigation, while differential GPS (DGPS) data were available for the calibration of the navigation data in ORI-347. An echo sounder provided the water depth profile along each seismic line. The seismic signals were recorded at a 4-ms sampling rate by three geophone channels installed in a gimbal mount. The data have an excellent signal-to-noise ratio despite some variation in source volume. The amount of data acquired along each line is about 25 M bytes for a period of about 4 to 5 hours of shooting.

The major data sets obtained during the OBS survey included raw OBS field data recorded on cartridge tapes, shot-time logs, navigation logs and bathymetry logs. Supplementary data recorded included clock-calibration files before deployment and after recovery of instruments, time, coordinates and water depths of OBS deployment and recovery, source positions with respect to navigation antenna, shot delay between logged shot time and actual air-gun firing, echo sounder depth and the time-depth conversion factor.

4. DATA PROCESSING

The OBS field data need pre-processing treatments to correct for errors and eliminate irregularities before they are processed. The calibrations of the OBS clock, shot time log, ship track, bathymetry and sampling rates are also necessary. Because of the inherent differences in the source-receiver geometry and the data content, the processing of OBS data is somewhat different from that of conventional seismic reflection. Some important differences are addressed in the following:

Shot locations: The precise locations of shots and OBS are important in a large-offset seismic survey. However, because raw navigation data are often fluctuant and not sufficiently stable, some additional processing of the navigation data, such as smoothing to eliminate glitches, is

necessary. Each shot location was computed in this study with the smoothed GPS (ORI-312) or DGPS (ORI-347) data based on a calibrated shot time log.

OBS location: The actual position of an OBS on the sea floor is slightly different from the location where it was deployed because of ocean currents encountered during its descent to the sea floor. Here, the direct water-wave arrival times were measured from the near range data and horizontal polarization was computed from the amplitude ratio H_1/H_2 of the two horizontal components of the geophones. The actual location, its orientation and the precise clock corrections could be determined simultaneously on the basis of arrival time of the direct water-wave signals, OBS deployed location and the clock calibrations one to two hours before deployment and after recovery of the OBS (Nakamura *et al.*, 1987).

Clock correction: Since each OBS works with its own internal clock which is independent of the clock on the shooting ship, the calibration of all clocks relative to a reference clock is necessary. Final clock adjustment can be made from the clock drift rates and the clock correction obtained with the OBS location as mentioned above. In turn, the shot delay and clock drift rate during data acquisition can be estimated.

A Standard SEG-Y format tape was generated by combining demultiplexed, decoded and time-corrected OBS seismic data with properly corrected shot-location and shot-time data. Horizontal-component data were rotated to radial and transverse directions based on the determined instrument orientation. Further processing of the data could be performed using available software packages. The record sections shown in Figures 3 to 6 were produced by stacking traces into uniformly spaced offset bins, band-pass filtering the traces and adjusting the gain.

5. ANALYSES AND INTERPRETATIONS

The line segments of the time-distance curve interpreted in the record sections (Figures 3 to 6) were used to deduce the velocity and thickness of each layer under the assumption that the velocity was constant and the refractor was horizontal in each layer. The slope of each line segment was the reciprocal of the velocity associated with the medium just below the boundary. When estimating the velocity and thickness of each layer by employing the travel-time equation of the head wave (e.g., Telford *et al.*, 1976), it was assumed that the velocity in the lower layer was higher than that in the upper layer. With only one OBS receiver generating useful seismic data set on each survey line we acquired, it was impossible to derive a unique structural solution from the unreversed data set. Nevertheless, the data did shed some light on certain aspects of the crustal structure which are discussed below.

5.1 Lines ORI-312 A, C and G

All three record sections (Figures 3, 4 and 5) were band pass filtered between 5 and 20 Hz and demonstrate clear refracted arrivals from boundaries of different velocity layers. Under the assumption of horizontal layering, the velocity structure estimated from these profiles is shown in Table 2. Line ORI-312A which was located to the east of the trench is essentially parallel to line ORI-312C located to the west of the trench (Figure 2), and the corresponding

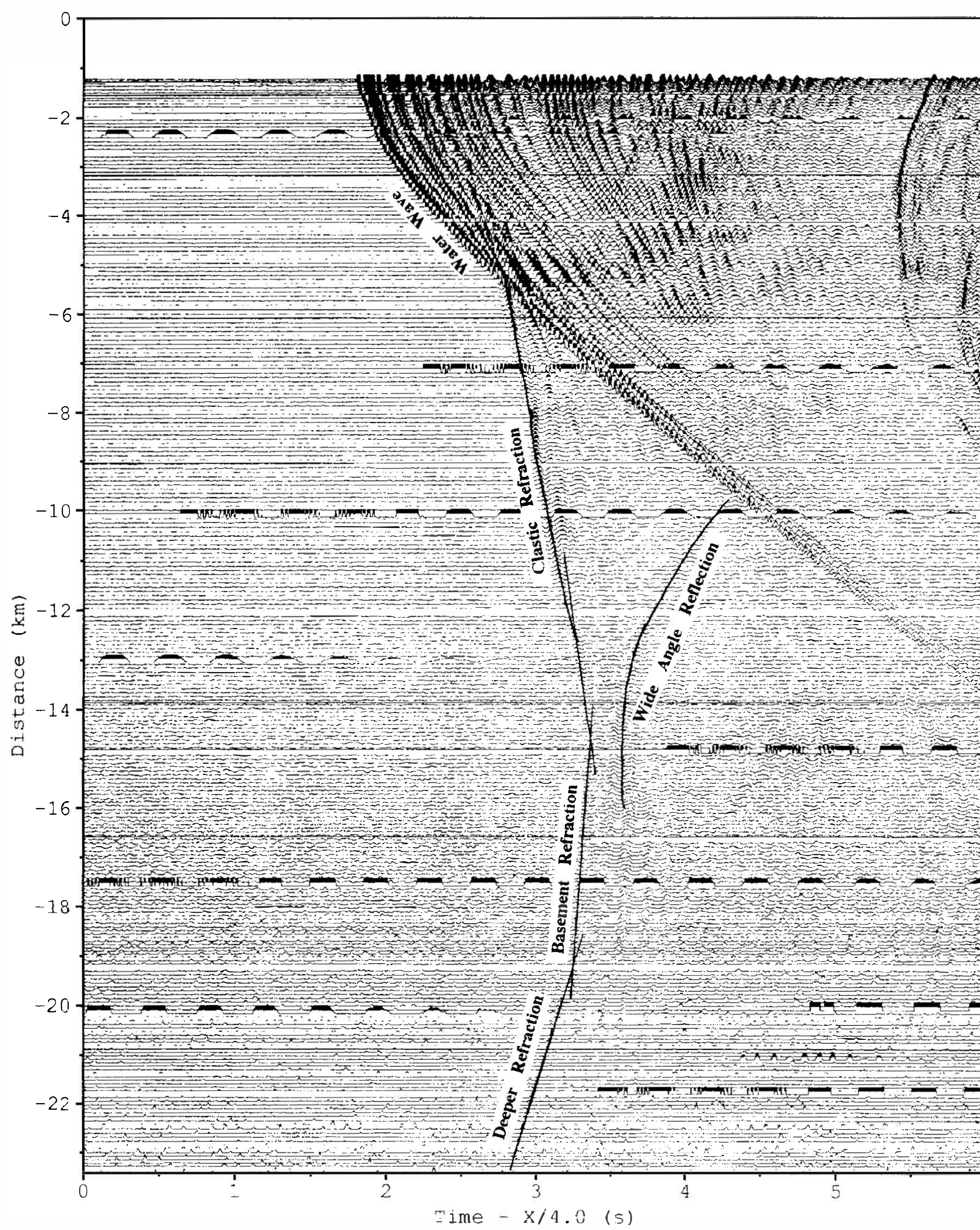


Fig. 3. Interpreted record section of line ORI-312A. This line was parallel to the trench in the arc-side. The basement refraction was very weak but observable. Travel time (in seconds) reduction of 4 km/sec was applied. OBS was located at 0 km. Note: The top curved arrivals close to 0 km are reflections from the most shallow sediments.

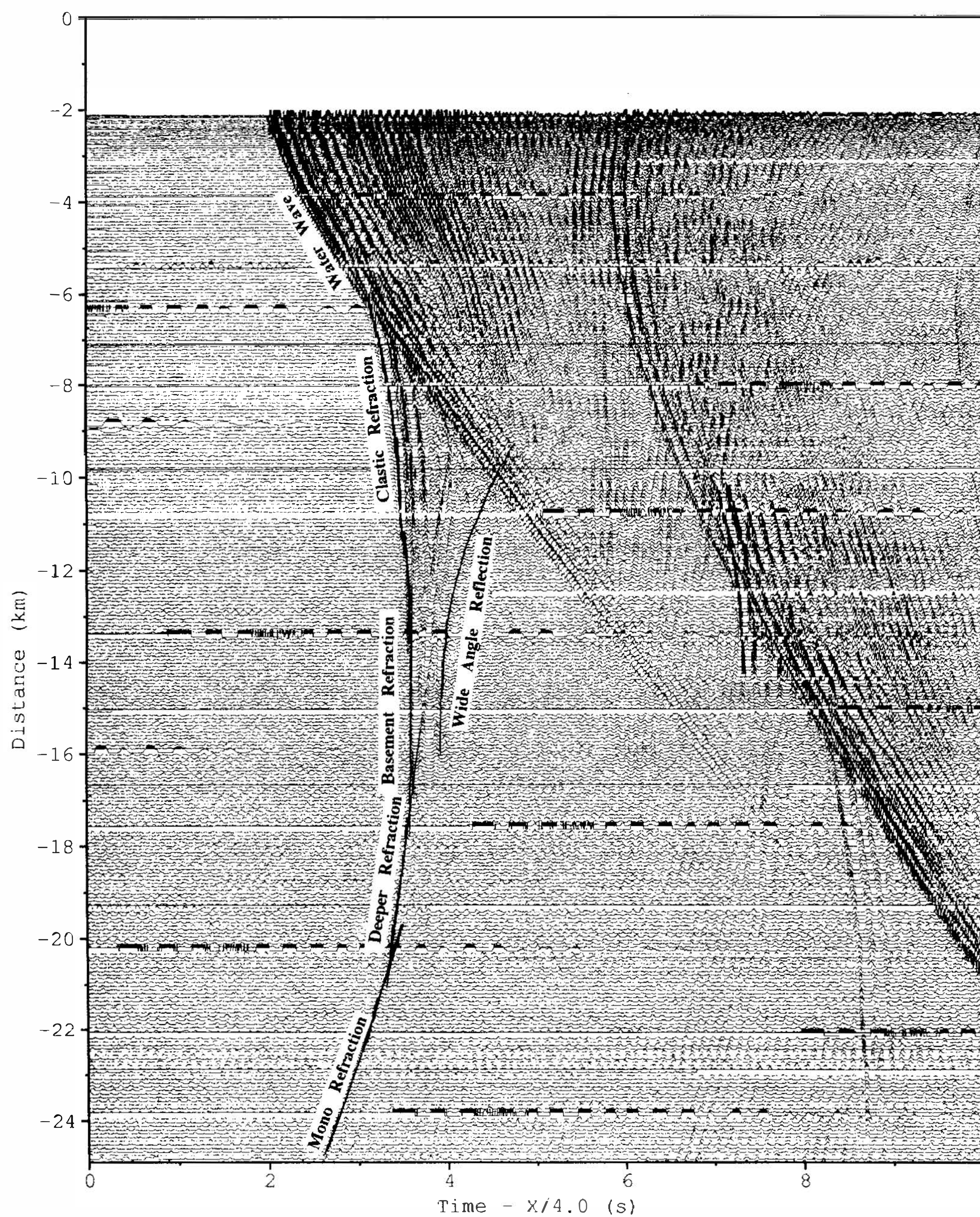


Fig. 4. Interpreted record section of line ORI-312C. This line was parallel to the trench and lay ocean side. The Moho refraction appears at a distance about 23 km from the OBS site which was located at 0 km. Travel time (in seconds) reduction of 4 km/sec was applied.

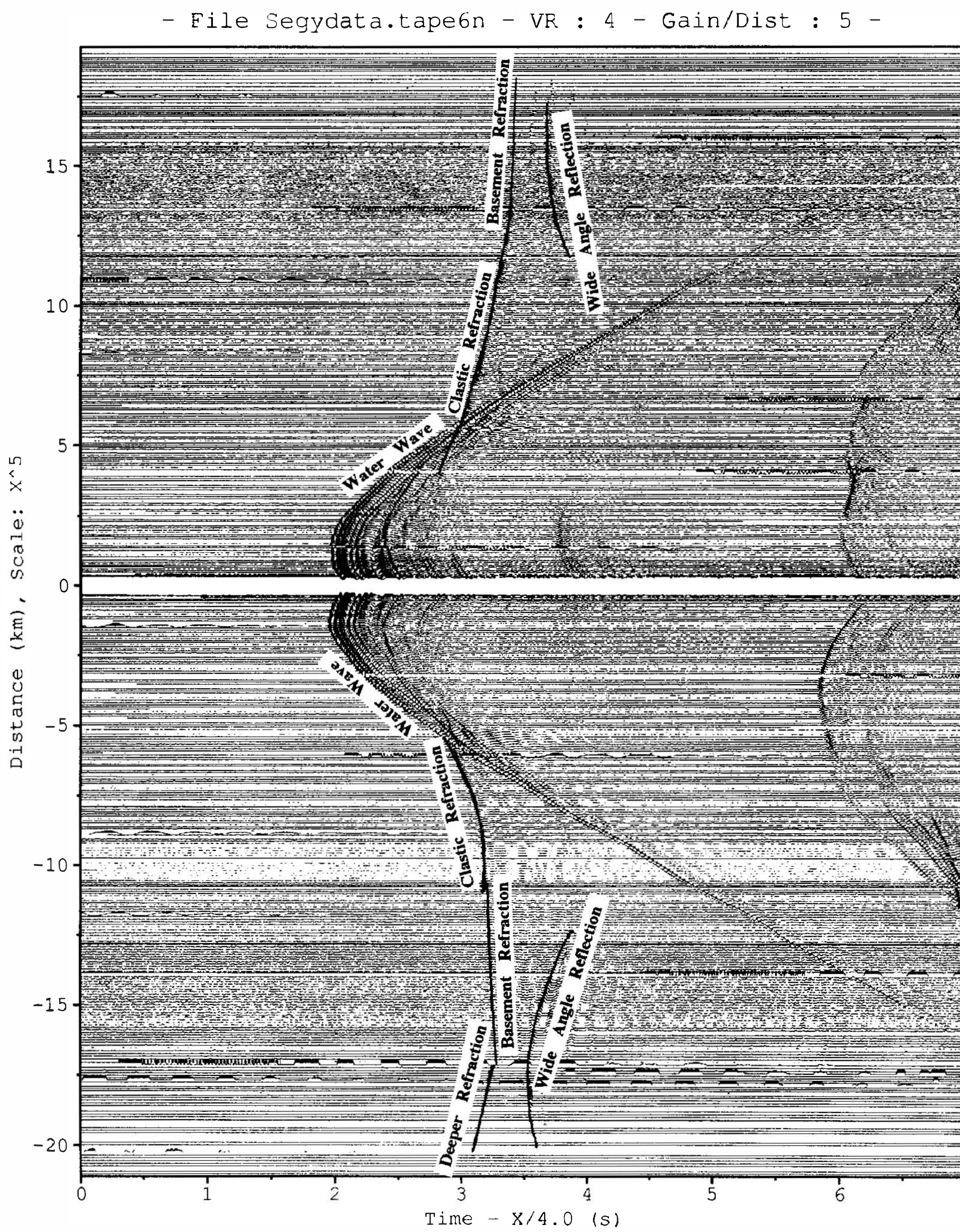


Fig. 5. Interpreted record section of line ORI-312G. This line ran across the trench. Travel time (in seconds) reduction of 4 km/sec was applied. The OBS site was located at 0 km.

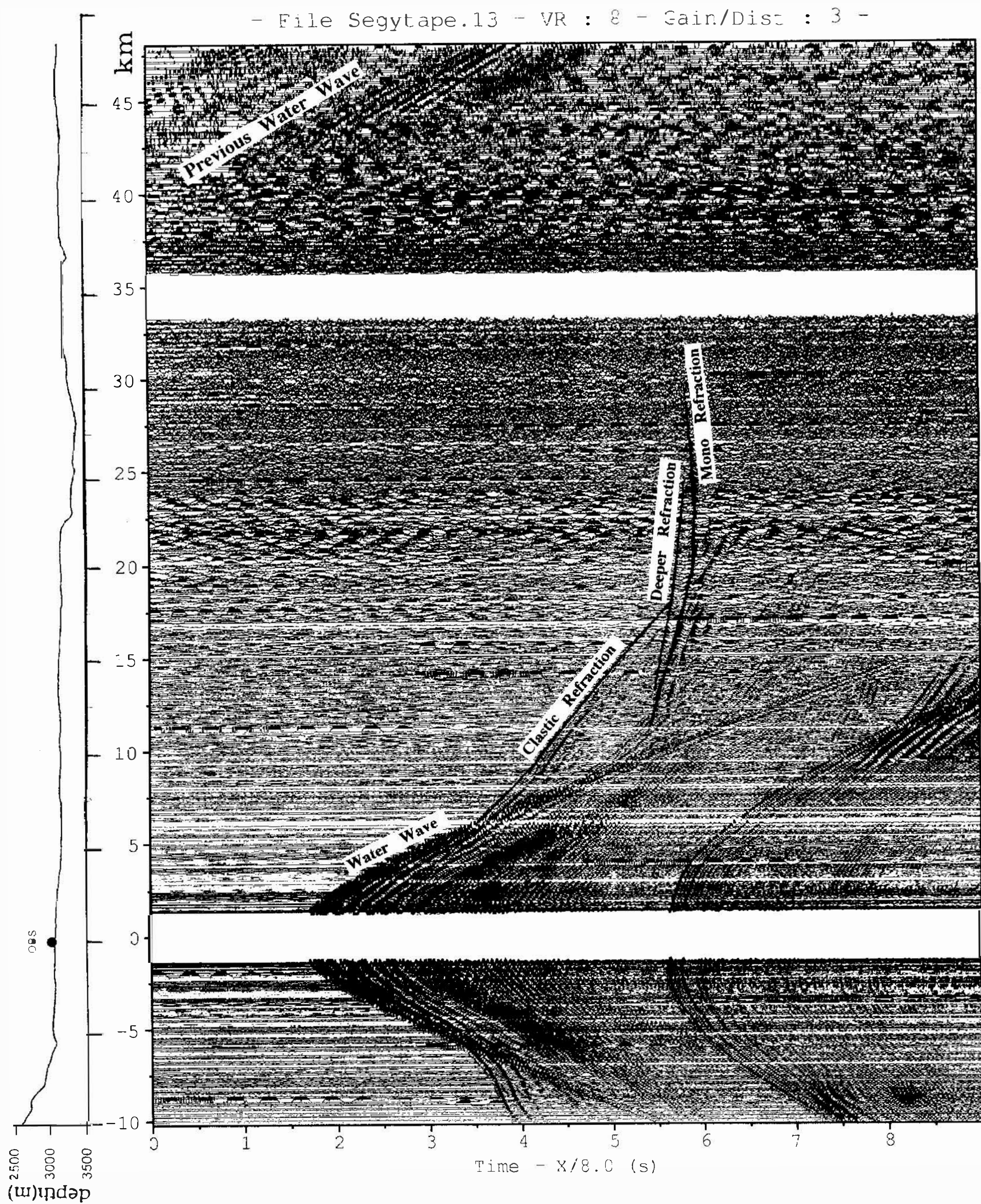


Fig. 6. Interpreted record section of line ORI-347. This line ran across the trench. Note: Travel time (in seconds) reduction of 8 km/sec was applied. There is a 20-minute gap of data due to a malfunction of the air-gun array. Bathymetry was added above the profile since no corresponding multi-channel seismic line was available.

layers are somewhat deeper in the eastern side than that in the western profile. While the OBSs on both the profiles ORI-312A and ORI-312C were deployed near the southern end, another OBS was located near the center of the profile ORI-312G. The refracted seismic arrivals from layer boundaries in either side of the trench along line ORI-312G is asymmetric (Figure 5). This may suggest that either the dipping layers were present or the local velocity structures were different along the line.

In addition to arrivals from sedimentary layers, oceanic basement, and deep crustal boundaries, Moho refraction was identified at a distance of about 23 km from the OBS along the profile ORI-312C (Figure 4). The corresponding velocity converted from the slope of the travel time curve exceeds 8.1 km/sec (Table 2 and Figure 10). The mantle velocity refracted at a depth of about 12 km below sea level provides crucial constraint in estimating the crustal thickness.

Table 2. Layered velocity models.

	ORI-312A		ORI-312C		ORI-312G east		ORI-312G west		ORI-347	
Layer	P Velocity km/s	Depth km								
0	1.50	2.96	1.50	3.19	1.50	3.12	1.50	3.12	1.50	3.00
1	1.70	3.47	1.70	3.60	1.70	3.56	1.70	3.64	1.70	3.27
2	2.46	3.72	2.05	3.85	2.28	3.91	2.37	3.85	1.98	3.91
3	3.17	4.78	2.87	5.95	3.11	4.69	3.01	4.73	3.29	4.22
4	3.67	5.65	4.00	8.41	3.59	6.10	3.49	6.26	3.36	6.92
5	4.00	9.59	6.34	11.78	4.01		4.06		4.26	9.18
6	6.44		8.16						6.32	12.20
7									8.14	

To refine the preliminary one-dimensional velocity model of Table 2 and to extend it into a two-dimensional one, a 2-D ray tracing technique was employed (Cerveny *et al.*, 1977; Luergert, 1993). Three multi-channel seismic profiles MCS320-37, MCS320-39 and MCS320-41, were acquired during cruise ORI-320 in the study area. The locations of these profiles almost coincided in locations with the OBS lines ORI-312G, C and A, respectively (Figure 2).

The profiles MCS320-39 and 320-41 were located at opposite sides of the Manila Trench. Their interpreted time sections show sedimentary layers dipping to the south (Figure 7 and 8). Localized fan-shape deposits were a common feature near the surface, deeper reflections were rather flat and continuous in MCS320-39. On the other hand, hummocky clinoforms characterized the seismic configuration in MCS320-41 and the seismic signals are weaker and less continuous throughout the sedimentary section. The profile MCS320-37, which crossed the trench, shows reflected horizons dipping steeper toward the arc (Figure 9). The acoustic basement was deeper than 6.5 sec and was progressively deeper toward the east.

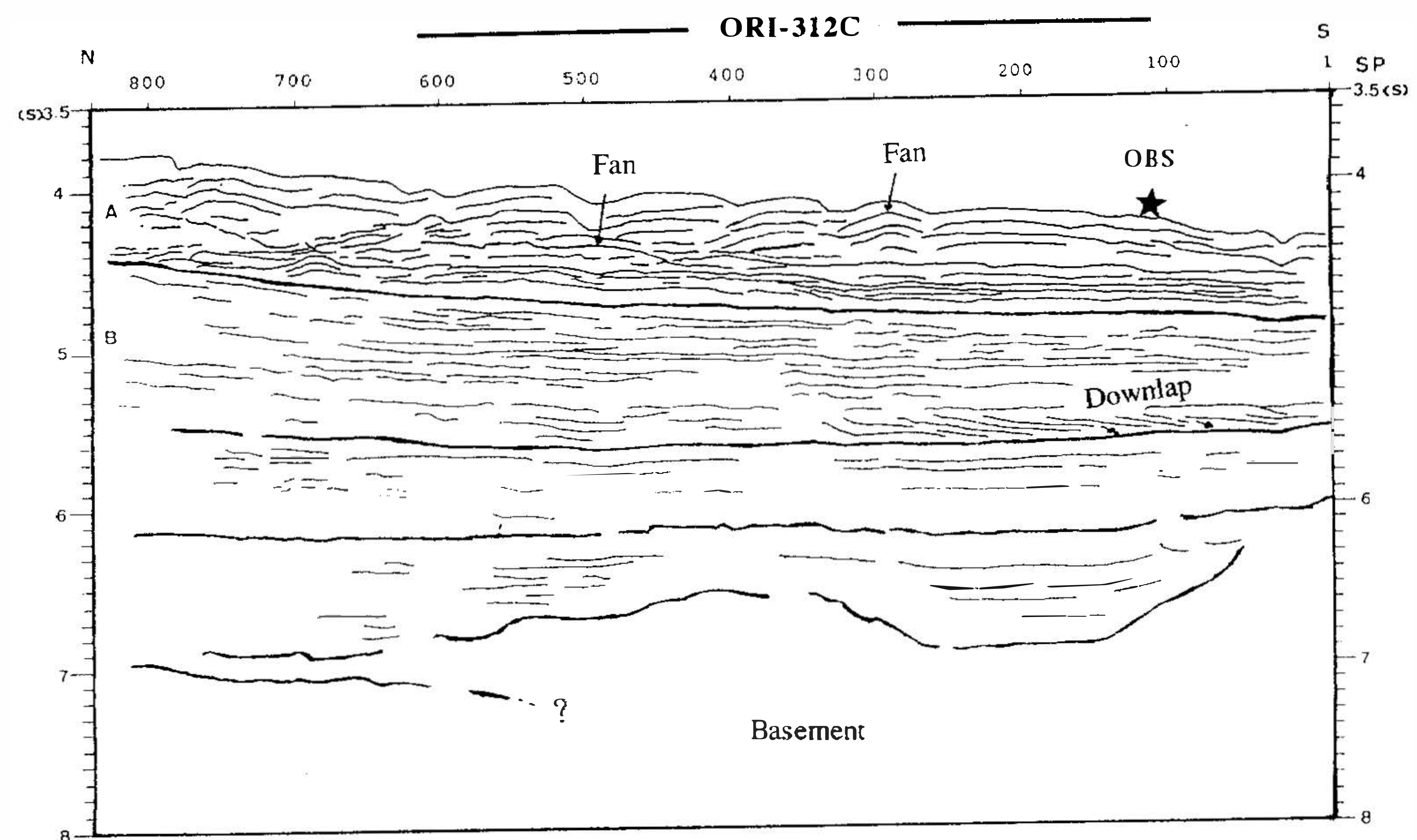


Fig. 7. Interpreted seismic line MCS320-39 (from Chen (1993)) with a projection of the OBS location. Note: The thick top line denotes the corresponding OBS profile.

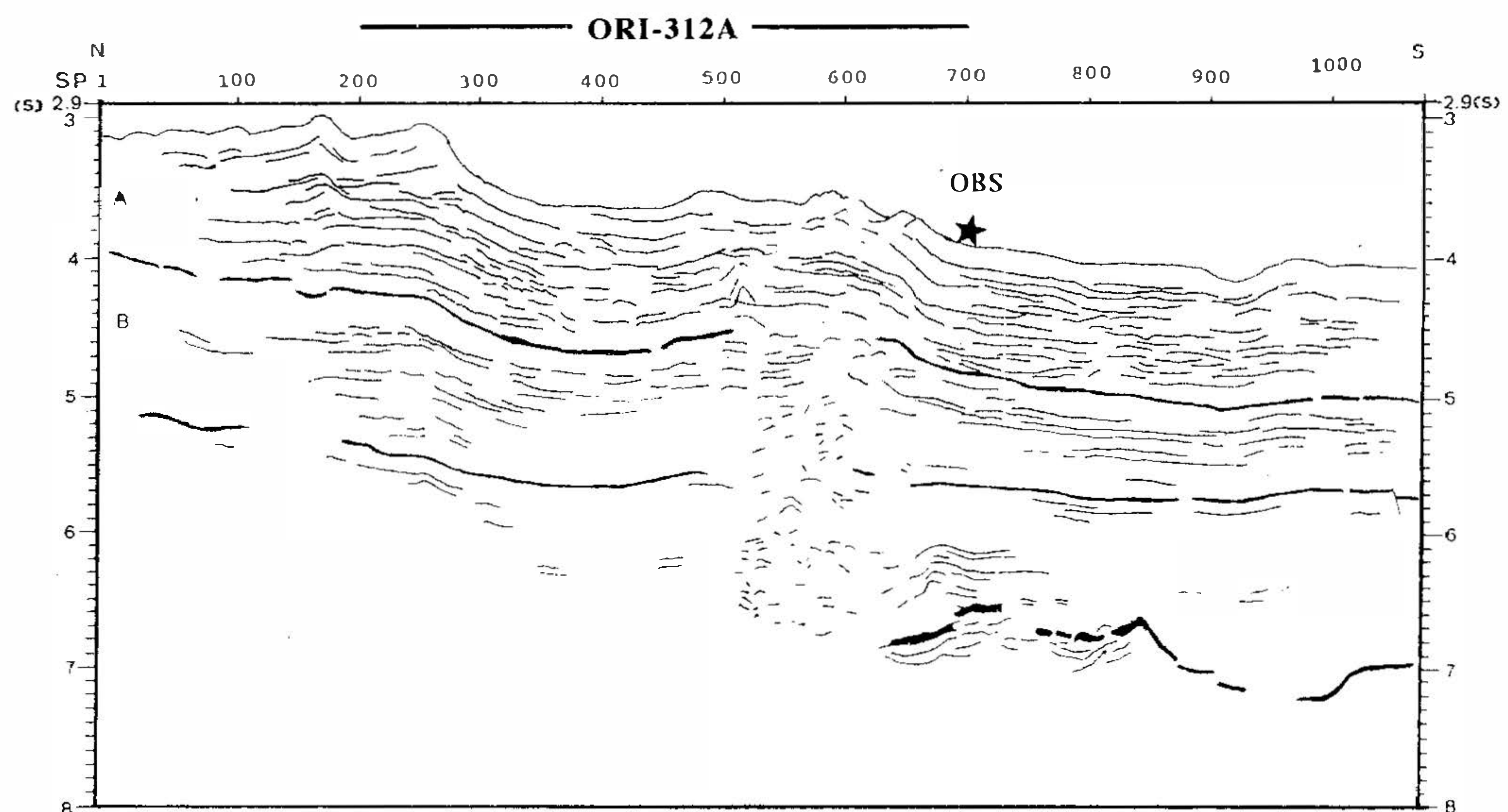


Fig. 8. Interpreted seismic line MCS320-41 (from Chen (1993)) with a projection of the OBS location. Note: The thick top line denotes the corresponding OBS profile.

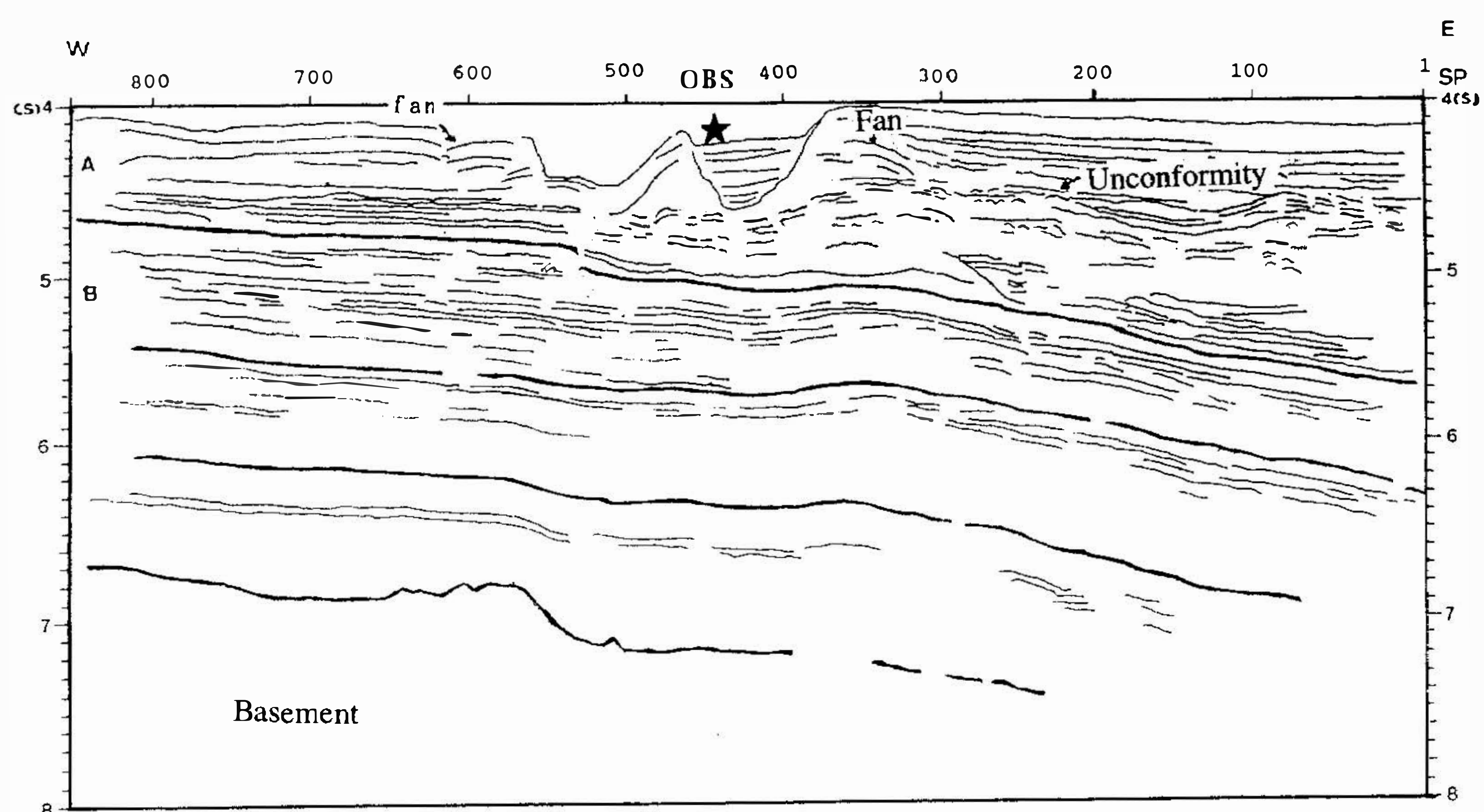


Fig. 9. Interpreted seismic line MCS320-37 (from Chen (1993)) with a projection of the OBS location. Note: This line and its corresponding OBS profile almost coincided with each other. The orientation of the display of this profile is the reverse of its counterpart shown in Figure 5.

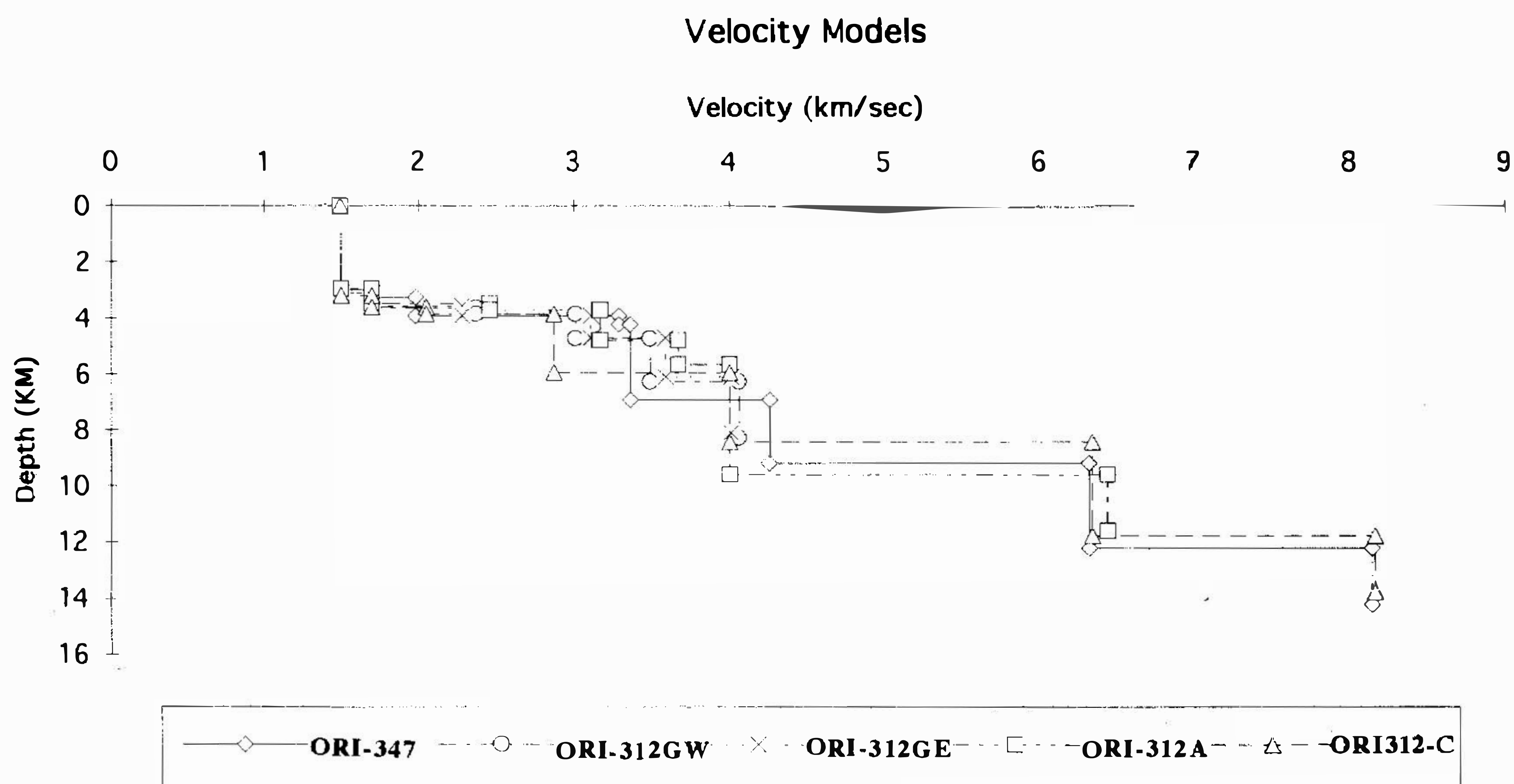


Fig. 10. 1-D layered velocity models corresponding to Table 2.

Sedimentary structures revealed from multi-channel seismic data (Chen, 1993) provide important constraints to the starting model of ray tracing. The theoretical travel time generated from the starting model was compared with the observed travel time, and the time difference between them was reduced by adjusting either the velocity structure or the layering attitude of the model. The model was, in fact, revised repeatedly until any further adjustment made no significant improvement, i.e., the overall time difference is essentially remained the same. Figures 11 to 13 show the final models, theoretical ray paths and theoretical arrival time against the observations in this study. Based on these final models, it is found that: (1) seismic velocity increases eastward (Figure 13), (2) the basement with velocity higher than 6 km/sec is deeper in the arc-side of the trench (Figure 11 vs. 12), and (3) the depth of the high velocity (8.17 km/sec) layer is down to 11.5 km below sea level (Figure 12).

5.2 Line ORI-347

This line is the most recent and longest (about 60 km) among all profiles acquired in this study. The OBS was deployed near the eastern end of the line. The record section is shown in Figure 6. Due to a malfunction of the air gun, there is a 20-minute, or 3-km, gap in the data set. However, clear first arrivals can be observed for offset less than 25 km. The arrivals of direct water-wave from previous shot at a distance beyond 40 km are also observed near the far end of the record. The first arrivals recognized in the ranges from 20 to 25 km is interpreted as signals refracted from the Moho discontinuity since it gives an apparent velocity of 8.14 km/sec. The estimated one-dimensional velocity structure along this profile is shown in Table 2 and Figure 10.

The 2-D ray tracing method was also applied to confirm the velocity structure of the ORI-347. Since there was no seismic reflection profile along this line, the authors began with a simplified flat layer model based on a one-dimensional velocity structure with a sea floor location constrained by bathymetric data. The resulting raypaths, models and theoretical arrival curves generally are not far from the initial model (Figure 14) with some finer structural variations. The velocity in layers deeper than 7 km remained uniform since no sufficient constraint for lateral variation was available. The result suggests that the Moho discontinuity lies at a depth of about 11.5 km which is compatible with that derived from the profile ORI-312C.

6. DISCUSSION

Due to operational negligence on the Omega clock system, there was a time difference of less than one minute between the Omega clock, which served as the reference time, and the GPS time during the data acquisition on both cruises. The computed location of each OBS profile based on the Omega time and a ship velocity of 5 knots may have been therefore shifted up to 150 meters from its actual position. However, the relative velocity structure converted from the processed seismic records in terms of the depth of layer thickness and its corresponding velocity remained essentially intact.

The velocity structures derived suggest that the Moho lies at a depth of about 11.5 km below sea level in the study area. This is in agreement with the crustal structure of the South China Sea in general (Taylor, 1980). Assuming the sedimentary layers represented by the

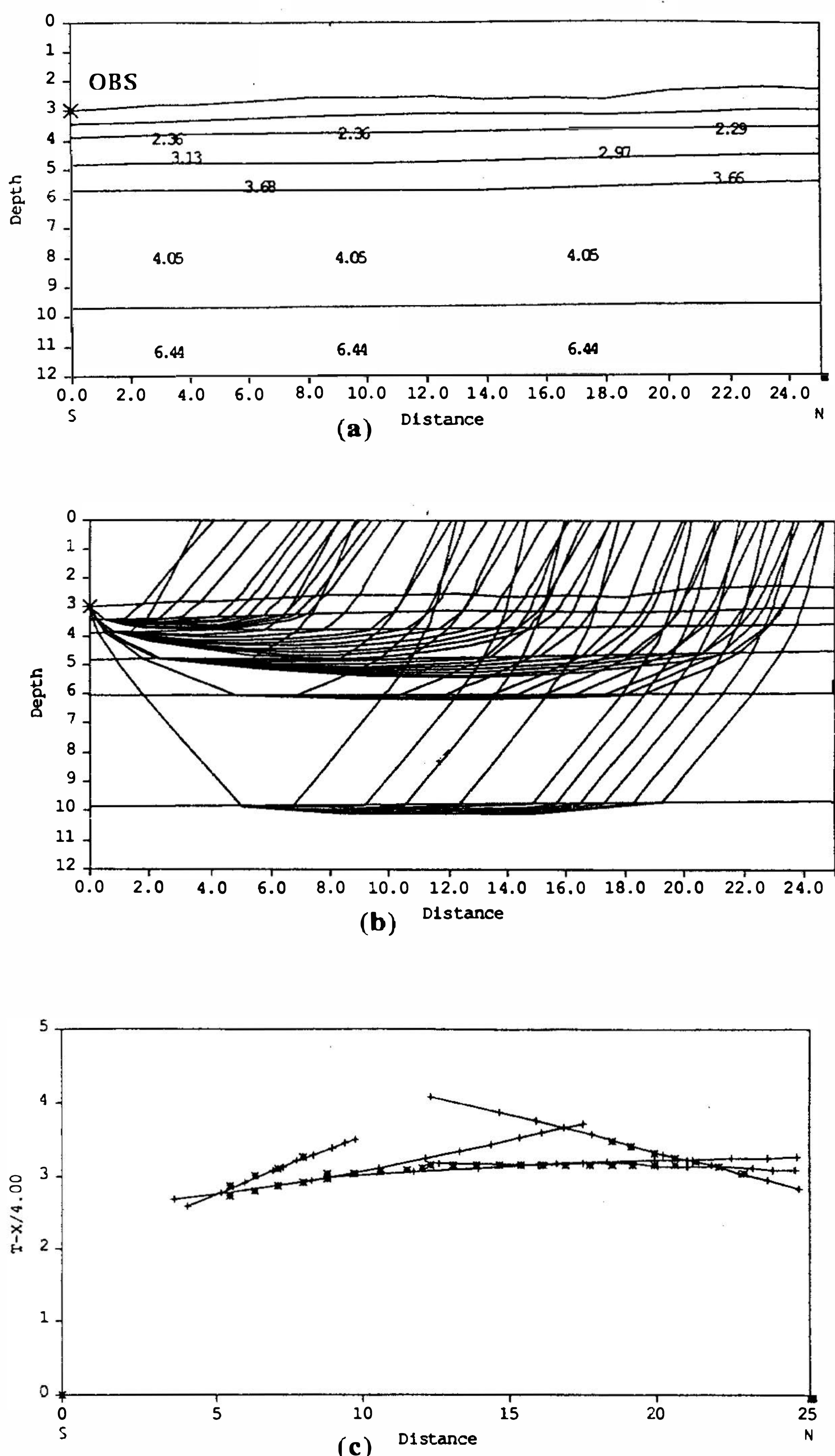


Fig. 11. (a) Final velocity structure model, (b) theoretical ray paths, and (c) theoretical travel time (solid lines with ticks) with their observed travel time picks (x) of the line ORI-312A.

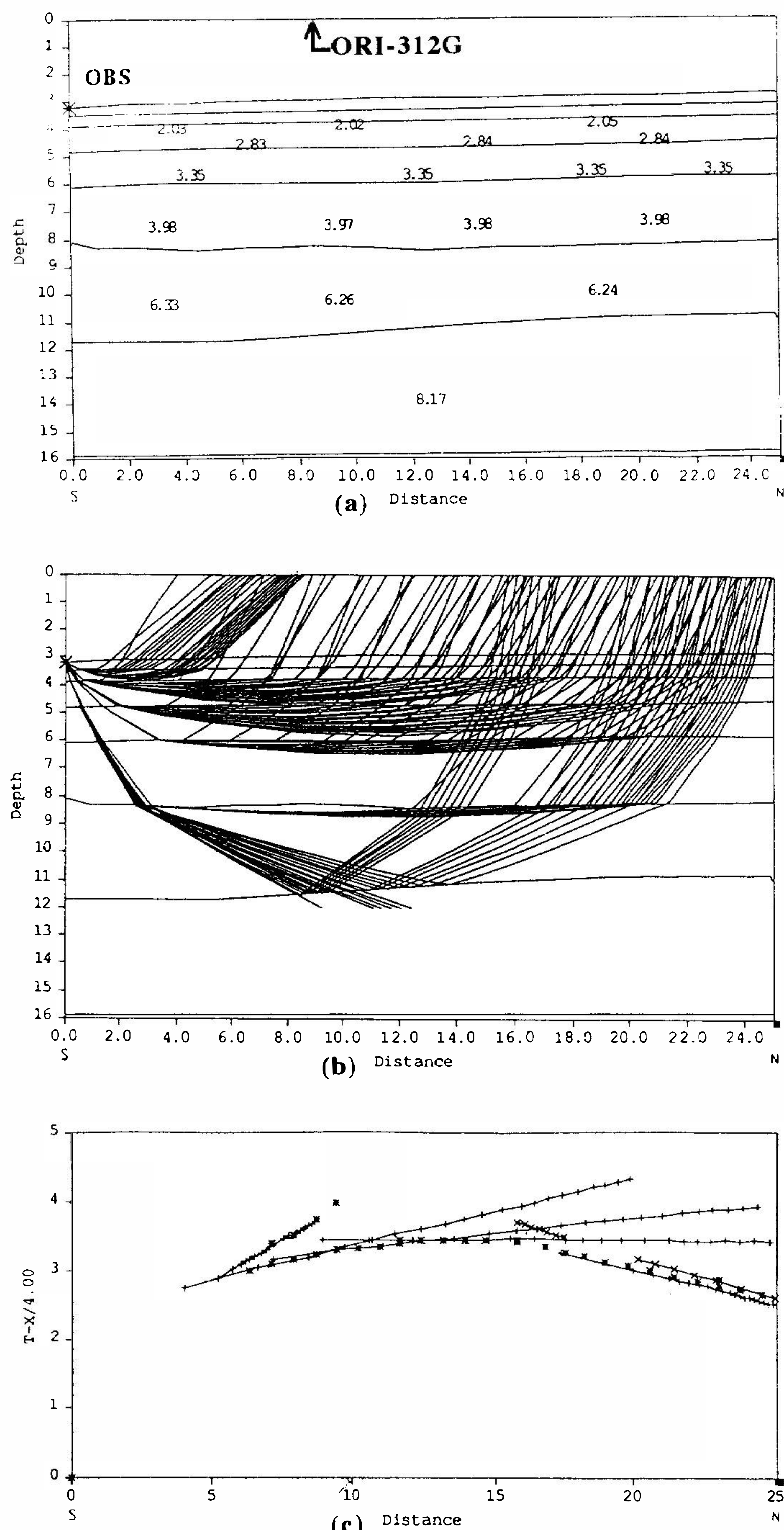


Fig. 12. (a) Final velocity structure model, (b) theoretical ray paths, and (c) theoretical travel time (solid lines with ticks) with their observed travel time picks (x) of the line ORI-312C. Note: The line ORI-312G is tied at a distance of 8.74 km along the profile.

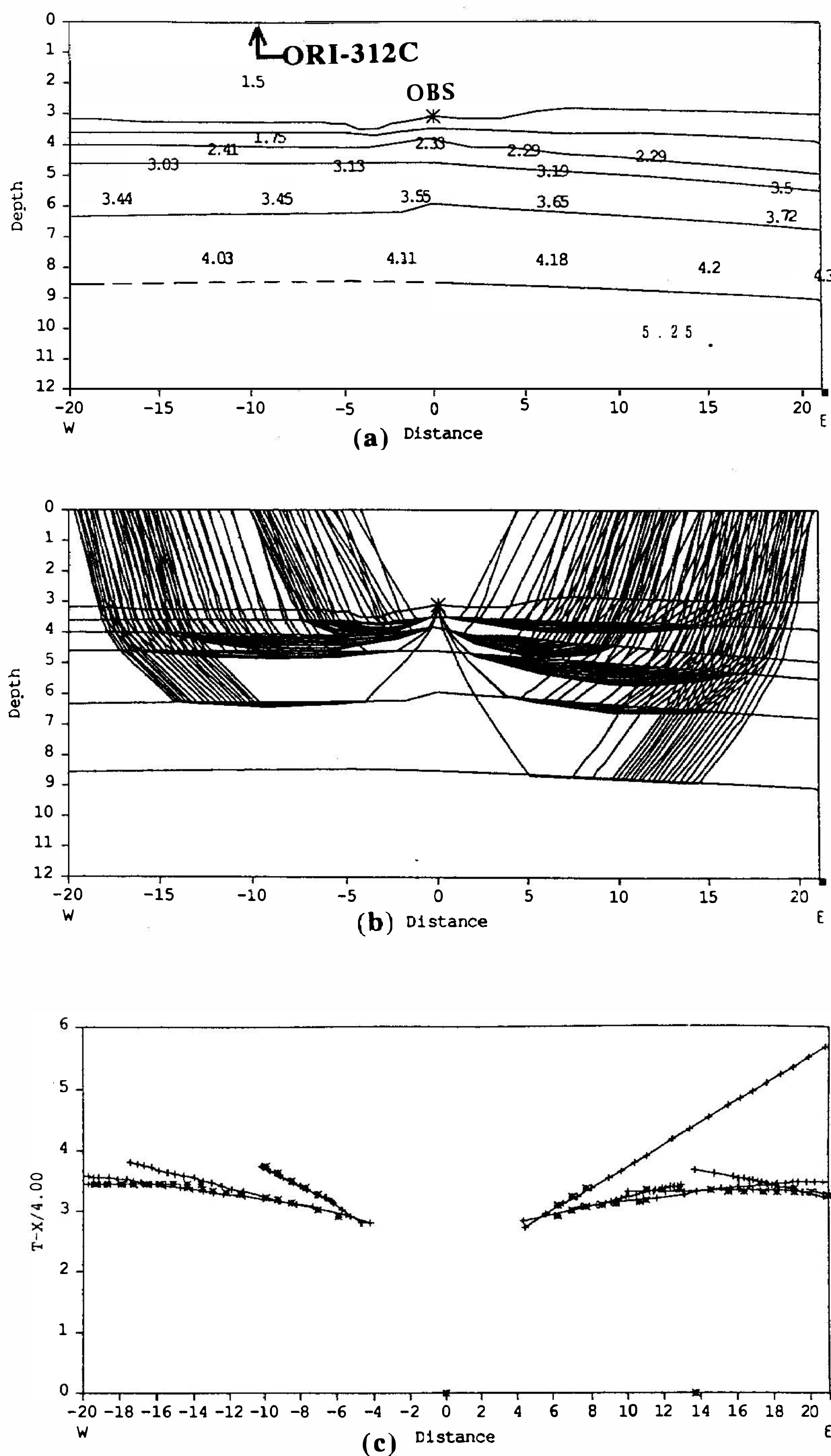


Fig. 13. (a) Final velocity structure model, (b) theoretical ray paths, and (c) theoretical travel time (solid lines with ticks) with their observed travel time picks (x) of the line ORI-312G. Note: The line ORI-312C is tied at a distance of 8.95 km along the profile.

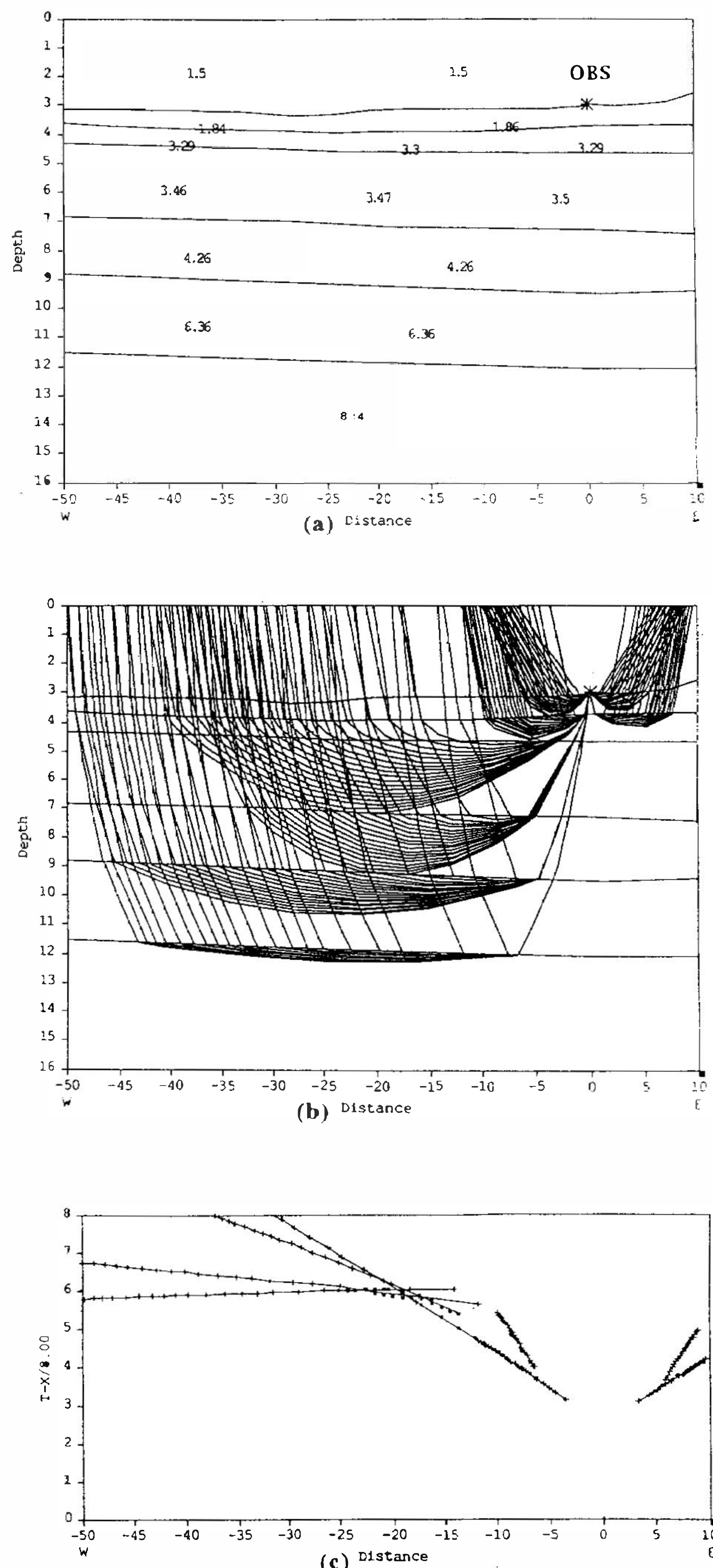


Fig. 14. (a) Final velocity structure model, (b) theoretical ray paths, and (c) theoretical travel time (solid lines with ticks) with their observed travel time picks (x) of the line ORI-347.

sections with a velocity lower than 4 km/sec and a thickness ranging from 2.7 to 3.7 km, the final models of ray tracing suggest that the depth to the basement is about 5.7-6.8 km, which is about 1.5 km deeper than the estimated depth of the magnetic basement (Liu *et al.*, 1992). The relatively thin crust, which ranges from 5.2 to 5.8 km in thickness, as revealed by the profiles ORI-312C and -347, further suggests the possibility of its having an oceanic nature. The thickness of the sedimentary layer is maintained at about 3 km or more along each profile.

The overall structure is pretty uniform along the profiles ORI-312A and -312C which are parallel to the trench. However, their velocity models are somewhat different. While the depth of the sedimentary layer with a velocity of less than 3.7 km/sec reaches a depth almost 6 km on both lines, the layer with a velocity higher than 6.2 km/sec is 1.5 km deeper along the eastern profile (Figures 8 and 9). The overall attitude of the profiles ORI-312G and -347 also show layers dipping to the east and is consistent with the concept of an eastward subduction of the South China Sea Basin crust.

7. CONCLUSIONS

Some seismic refraction data from OBS experiments are presented so as to construct velocity models in the vicinity of the Manila Trench southwestern offshore Taiwan. The apparent velocity of the upper mantle based on record sections of the ORI-312C and -347 is close to 8.1 km/sec at depth exceeding 11 km. The thickness of the sedimentary layer is 3 to 4 km and remains about the same within 10 km on either side of the trench. The igneous crustal structure revealed by the models of the profiles ORI-312A and -312C shows that it is thicker east of the Manila Trench. The thin crust observed along the profiles ORI-312C and -347 at the west side of the trench is only 5 to 6 km in thickness and is concluded to be oceanic in origin.

Acknowledgments The authors thank the captain and crew of the *R/V Ocean Researcher I* for their help in acquiring the geophysical data. Appreciation is also extended to Dr. Yosio Nakamura who offered some constructive suggestions. The authors also benefited from critical comments by two anonymous reviewers. This work was supported by the National Science Council grants NSC81-0209-M-019-04 and NSC82-0209-M-019-008.

REFERENCES

- Barrier, E., and J. Angelier, 1986: Active collision in eastern Taiwan: the coastal range. *Tectonophysics*, **125**, 39-72.
- Biq, C. C., 1973: Kinematic pattern of Taiwan as an example of actual continent-arc collision. Rept. in Seminar on Seismology, US-ROC Cooperative Sci. Prog., 21-26.
- Biq, C. C., 1977: The Kenting melange and the Manila Trench. *Proc. Geol. Soc. China*, **20**, 119-122.
- Bott, M. H. P. 1982: The interior of the earth, its structure, constitution and evolution (2nd Ed.), Edward Arnold, London, 403pp.
- Bowin, Carl, R. S. Lu, C. S. Lee, and H. Schouten, 1978: Plate convergence and accretion in

- the Taiwan-Luzon region. *Am. Asso. Petrol. Geol. Bull.*, **62**, 1645-1672.
- Cerveny, V., I. A. Molotkov, and I. Psencik, 1977: Ray methods in seismology. Charles University, Prague, 57-120.
- Chen, A. T., Y. Nakamura, and L. W. Wu, 1992: Investigating deep crustal structure in the northeastern south China Sea and Taiwan Strait using ocean bottom seismographs. *Acta Geol. Taiwanica*, **30**, 145-148.
- Chen, A. T., Y. Nakamura, and L.W. Wu, 1994: Ocean bottom seismographs: instrumentation and experimental technique. *TAO*, **5**, 109-119.
- Chen, J. 1993: Investigation of the transition zone and the northern extension of the Manila Trench offshore southwestern Taiwan. Master thesis, National Taiwan Ocean University, 93pp. (in Chinese).
- Huang, C. Y., C. T. Shyu, S. B. Lin, T. Q. Lee and D. D. Sheu, 1992: Marine geology in the arc-continent collision zone off southeastern Taiwan: implication for the late Neogene evolution of the Coastal Range. *Marine Geol.*, **107**, 183-212.
- Huang, I. L., L. S. Teng, C. S. Liu, D. L. Reed, and N. Lundberg, 1992: Structural styles of offshore southwestern Taiwan. *EOS Trans. AGU*, **73**, p.539.
- Jahn, B. M., F. Martineau, J. J. Peucat, and J. Corniche, 1986: Geochronology of the Tananao schist complex, Taiwan, and its regional tectonic significance. *Tectonophysics*, **125**, 103-126.
- Lee, T. Y., C. H. Tang, J. S. Ting, and Y. Y. Hsu, 1993: Sequence stratigraphy of the Tainan Basin, offshore southwestern Taiwan. *Petrol. Geol. Taiwan*, **28**, 119-158.
- Lin, M. T. and Y. B. Tsai, 1981: Seismotectonics in the Taiwan-Luzon area. *Bull. Inst. Earth Sci., Academia Sinica*, **1**, 51-82.
- Liu, C.S., S.Y. Liu, B.Y. Kuo, N. Lundberg and D. L. Reed, 1992: Characteristics of the gravity and magnetic anomalies off southern Taiwan. *Acta Geol. Taiwanica*, **30**, 123-130.
- Liu, C. S., S. Y. Liu, G. S. Song, C. T. Shyu, H. S. Yu, L. T. Chiao, C. S. Wang, and B. Karp, 1996: Digital bathymetry data offshore Taiwan. Program with Abstracts, 1996 Annual Meeting of Geol. Soc. China, 420-425.
- Luergert, J. H., 1993: MacRay (2), interactive two-dimensional seismic raytracing for the Macintosh. U.S.G.S. Open File Report, 92-356.
- Lundberg, N., D. L. Reed, and C. -S.. Liu, 1991: The submarine propagating tip of the Taiwan collision, shallow crustal structure and orogenic sedimentation. Taicrust Workshop Proceedings, **93**-102.
- Nakamura, Y., P. L. Donoho, P. H. Roper, and P. M. McPherson, 1987: Large-offset seismic surveying using ocean-bottom seismographs and air guns, Instrumentation and field technique. *Geophysics*, **52**, 1601-1611.
- Reed, D. L., N. Lundberg, C.-S. Liu, and B.-Y. Kuo, 1992: Structural relations along the margins of the offshore Taiwan accretionary wedge: implications for accretion and crustal kinematics. *Acta Geol. Taiwanica*, **30**, 105-122.
- Seno, T., 1977: The instantaneous rotation vector of the Philippine Sea plate relative to the Eurasian plate. *Tectonophysics*, **42**, 209-226.
- Seno, T., and K. Kurita, 1978: Focal mechanisms and tectonics in the Taiwan-Philippine

- region. In: S. Uyeda, R. W. Murphy and K. Kobayashi (Eds.), *Geodynamics of the Western Pacific, J. Phys. Earth Suppl. Issue, 26*, 247-263.
- Suppe, J. 1988: Tectonics of the arc-continent collision on both sides of the South China Sea: Taiwan and Mindoro. *Acta Geol. Taiwanica, 26*, 1-18.
- Taylor, B., and D. E. Hayes, 1980: The tectonic evolution of the South China Basin. In: D. E. Hayes (Ed.), *The tectonic and geologic evolution of southeast Asian seas and islands. AGU Monogr., 23*, 89-104.
- Telford, W. M., L. P. Geldart, R. E. Sheriff and D. D. Keys, 1976: *Applied Geophysics*. Cambridge University Press, Cambridge, England, 860pp.
- Teng, L. S., 1990: Geotectonic evolution of late Cenozoic arc-continent collision in Taiwan. *Tectonophysics, 183*, 57-76.
- Wu, F. T., 1978: Recent tectonics of Taiwan. *J. Phys. Earth Suppl. Issue, 26*, 265-297.
- Yu, S. B., and H. Y. Chen, 1994: Global positioning system measurements of crustal deformation in the Taiwan arc-continent collision zone. *TAO, 5*, 477-498.